Journal of the Optical Society of Korea
Vol. 12, No. 3, September 2008, pp. 131-135

DOI: 10.3807/JOSK.2008.12.3.131

# Computational Integral Imaging Reconstruction of 3D Object Using a Depth Conversion Technique

Dong-Hak Shin*

*Dept. of Visual Contents, Graduate School of Design & IT, Dongseo University San 69-1, Churye-2-Dong, Sasang-Gu, Busan 617-716, Korea*

Eun-Soo Kim

*Dept. of Electronics, Kwangwoon University, 447-1, Wolge-Dong, Nowon-Gu, Seoul 139-701, Korea*

(Received May 21, 2008 : revised July 1, 2008 : accepted July 30, 2008)

Computational integral imaging (CII) has the advantage of generating the volumetric information of the 3D scene without optical devices. However, the reconstruction process of CII requires increasingly larger sizes of reconstructed images and then the computational cost increases as the distance between the lenslet array and the reconstructed output plane increases. In this paper, to overcome this problem, we propose a novel CII method using a depth conversion technique. The proposed method can move a far 3D object near the lenslet array and reduce the computational cost dramatically. To show the usefulness of the proposed method, we carry out the preliminary experiment and its results are presented.

*Keywords* : 3D display, integral imaging, computational reconstruction, depth conversion, lenslet array

*OCIS codes* : (100.6890) Three-dimensional image processing; (110.6880) Three-dimensional image acquisition

## I. INTRODUCTION

Integral imaging is a promising technique for 3D imaging and visualization. It can record and reconstruct 3D objects with full parallax, continuous viewing points and the use of white light [1-6]. However, there are several problems to be solved such as low resolution, narrow viewing angle, and pseudoscopic images. In order to overcome the pseudoscopic problem of reversed depth, some techniques on depth conversion have been reported such as two-step integral photography [7], gradient-index lens array [8] and computer-generated integral imaging [9-11].

Recently, for 3D visualization and recognition using integral imaging, a concept of computational integral imaging (CII) has been proposed [12-14]. This CII is composed of the optical pickup process and the volumetric computational reconstruction (VCR). In the optical pickup process, 3D object is recorded as the elemental image array (EIA) through a lenslet array. In the VCR process, the EIA is digitally reconstructed by using a computer in order to obtain volumetric 3D images. CII has several problems to be solved such as a poor resolution of the reconstructed image [6,13], high computational cost [14], reconstruction limitation of far 3D objects [15], and so on.

Among them, to solve the problem for far 3D objects, a study using an additional lens was reported [15]. However the enhancement was obtained by using an additional lens device. In this paper, we propose a computational method without an optical device. In the proposed CII method, we apply a depth conversion technique to the conventional system. This function of depth conversion provides us with moving a far object near a lenslet array and then reducing the computational cost of the reconstructed 3D image for a far object. To show the usefulness of the proposed method, we carry out the preliminary experiment. For our depth conversion technique in the experiment, the smart pixel mapping (SPM), which is one of computational depth conversion schemes, is used. First, the EIA of 3D objects is picked up by using an

*Corresponding author: shindh2@dongseo.ac.kr

optical pickup process. In order to generate a new set of EIA, SPM algorithm is applied to the EIA. Reconstruction for EIA is done by using a VCR technique. We finally compare the reconstructed images for the proposed method and the conventional method.

## II. CII METHOD USING DEPTH-CONVERSION TECHNIQUE

Figure 1 shows the diagram of the proposed CII method using a depth conversion technique. Compared with the conventional CII, we use a depth conversion technique additionally to obtain a depth-converted EIA. First, EIA of 3D objects are recorded through the pickup process. In order to generate a depth-converted EIA, a depth conversion technique is applied to the recorded EIA. With the depth-converted EIA, a reconstruction output image (ROI) is calculated computationally by using the VCR process. Also the depth conversion can be performed computationally.

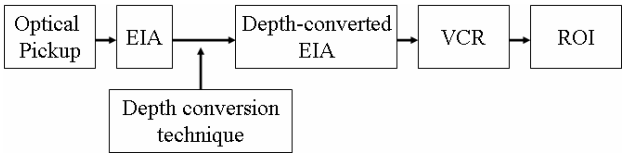


FIG. 1. Blockdiagram of the proposed CII method

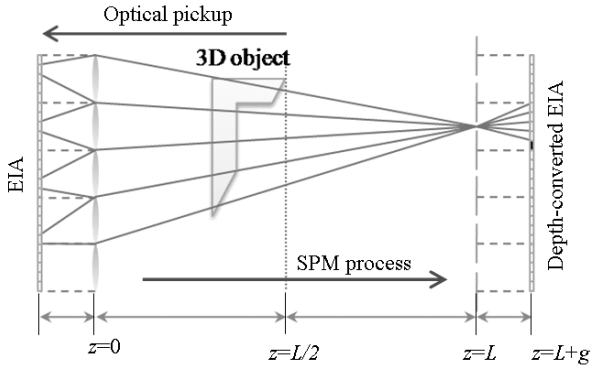


(a)

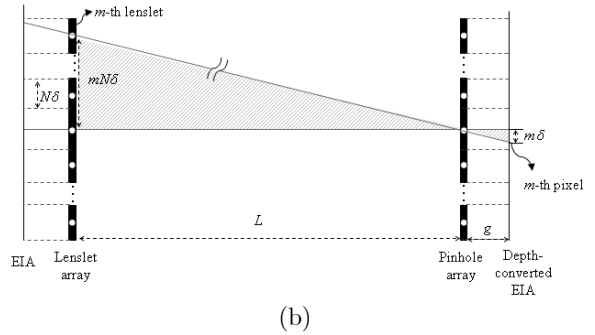


(b)

FIG. 2. (a) Principle of SPM (b) Ray diagram for calculating the distance $L$

For the depth conversion technique used in this paper, we can consider the previous computational methods [9-11]. We use the SPM algorithm [11] in order to show the usefulness of the depth conversion effect. SPM is a computational pseudoscopic-to-orthoscopic (PO) conversion technique which is able to produce undistorted real, orthoscopic integral images. The original EIA obtained in the optical pickup process is applied with the SPM algorithm to form a depth-converted EIA. Figure 2 shows the mapping process of the SPM algorithm based on the computational model. Let us consider $M$ elemental images which are composed of $N$ pixels per each elemental image. The lenslet array is located at $z=0$ and $g$ is the distance between the lenslet array and EIA. For SPM process, a virtual pinhole array should be located at the fixed distance $L$ between the lenslet array and virtual pinhole array as shown in Fig. 2(b). Figure 2(b) shows the ray analysis to calculate the condition to avoid the typical aliasing problem [11], which prevents the synthesis of proper depth-converted EIA. We suppose a ray mapping between $m$-th lenslet and $m$-th pixel in the depth-converted EIA. In Fig. 2(b), $\delta$ is the pixel size and then the length of the elemental image is $N\delta$. The condition for the distance $L$ is easily derived from two adjacent triangles shown in Fig. 2(b). That is, the distance $L$ is the product of $N$ to $g$. The depth-converted EIA is synthesized in the pickup plane at $z=L+g$. Under the limited condition of $L=Ng$, the SPM algorithm for the one-dimensional case is formulated as

$$T_{i,j}=O_{k,l} \tag{1}$$

where

$$l=(M+1)-j \quad \text{and} \quad k=\begin{cases} i+M/2-j & \text{if } M \text{ is even.} \\ i+(M+1)/2-j & \text{if } M \text{ is odd} \end{cases}$$

Here, $T$ and $O$ are the depth-converted EIA and original EIA, respectively. The subscripts $i$ and $k$ correspond to the elemental image number and $j$ and $l$ are the pixel number in the given elemental image, respectively. From Eq. (1), we can simply calculate the depth-converted EIA using only digital process. This process is not consumed in the respect of the computational cost because of a simple pixel mapping.

Next, the depth-converted EIA is used to reconstruct 3D image using the VCR process as shown in Fig. 3. The reconstruction process of the VCR can extract voxel information at coordinates ($x$, $y$, $z$) for the 3D object from the EIA. The principle of the VCR is as follows. As shown in Fig. 3(b), we consider one-dimensional notation and $M$ elemental images located at the distance $g$ from the pinhole array. The extension to two-dimensional is straightforward. Let $E_n(x)$ be the $n$-th elemental image,

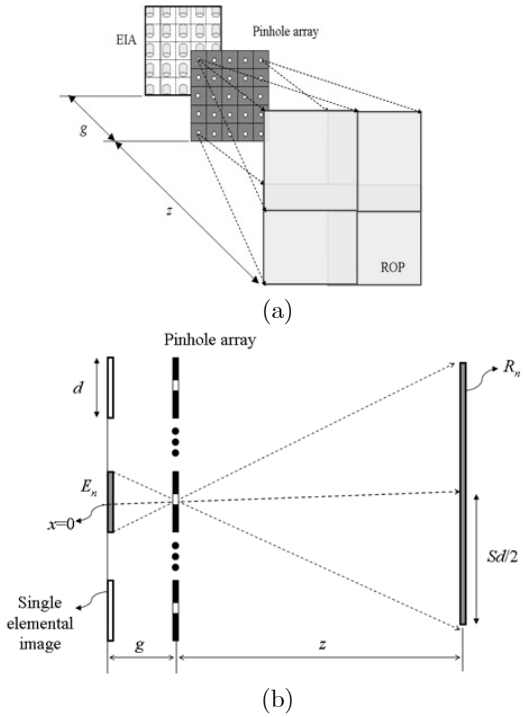


FIG. 3. Principle of VCR (a) Conceptual diagram (b) Ray analysis

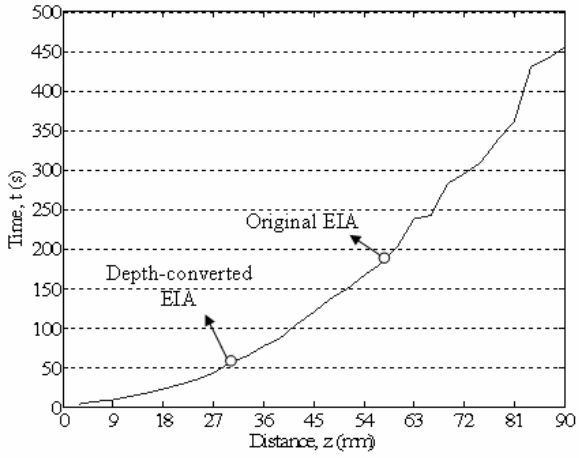


FIG. 4. Computational time of VCR process according to the distance $z$

and $R_n(x, z)$ be the reconstructed plane image at the reconstructed output plane (ROP) $z$. Here integer $n = -M/2$ to $M/2$. As shown in Fig. 3, $R_n(x, z)$ is represented in terms of elemental image $E_n$. Then it is given by

$$R_n = \frac{1}{S} E_n\left( nd - \frac{x - nd}{S} \right) \quad \text{for} \quad d(n - \frac{S}{2}) \le x \le d(n + \frac{S}{2}) \tag{2}$$

where $d$ is the size of the elemental image in the lateral direction and $S = z/g$ is a magnification factor according to the distance. The reconstructed 3D image at $z$ is the summation of all the inversely mapped elemental images and is represented by

$$R(x, z) = \sum_{n=-M/2}^{M/2} R_n(x, z) \tag{3}$$

For $S > 1$, inversely mapped images at ROP are overlapping each other. ROP can be normalized to reduce the effect of the intensity irregularities [13]. However, the conventional VCR suffers from the problem of high computational cost as the distance between lenslet array and ROP increases. In other words, the computational time of VCR is mainly related to the magnification factor $S$. To explain the computational cost of the VCR process, we can consider the pixel number to be processed. In general, the VCR process is classified into two steps: magnification and superimposition as shown in Fig. 3(a). Then, the pixel number to be processed in each step can be calculated. Assume that each elemental image with $N \times N$ pixels is magnified using the copy operation by $S$ times and $K \times K$ elemental images are repeated. Both magnification and superimposition steps should deal with the $K^2 \times (S^2 N^2)$ pixels. The total pixel number to be processed in the VCR process is given by

$$C_{pixel} = 2K^2 \cdot (S^2 \times N^2) \tag{4}$$

Since $K$ and $N$ are fixed numbers for given elemental images in Eq. (4), the total pixel number is linearly proportional to the square of magnification factor $S$. Therefore, it is seen that the computational cost increases dramatically as $S$ increases. An example of the computational times according to the distance is shown in Fig. 4. We see that the time increases dramatically with increasing distance. Therefore, we can see that reducing the ROP distance of 3D object is a good solution of computational cost problem.

## III. EXPERIMENTS AND RESULTS

To show the usefulness of the proposed method, we carried out the preliminary experiments. Figure 5(a) shows an experimental setup for optical pickup. The '3D' character pattern is used as a 3D object and captured by using a capture device. The optical lenslet array has $30 \times 30$ square lensets and each lenslet size is measured to be 1.08 mm. The focal length of the lenslet is measured to be $g = 3$ mm. In the experiment the distance between the character pattern and the lenslet array was $z = 60$ mm. The captured EIA was shown in Fig. 5(b). The size of each elemental image was $30 \times 30$ pixels. With this condition, we modeled the system structure for SPM where $M = N = 30$ and $L = 90$ mm as shown in Fig. 2.

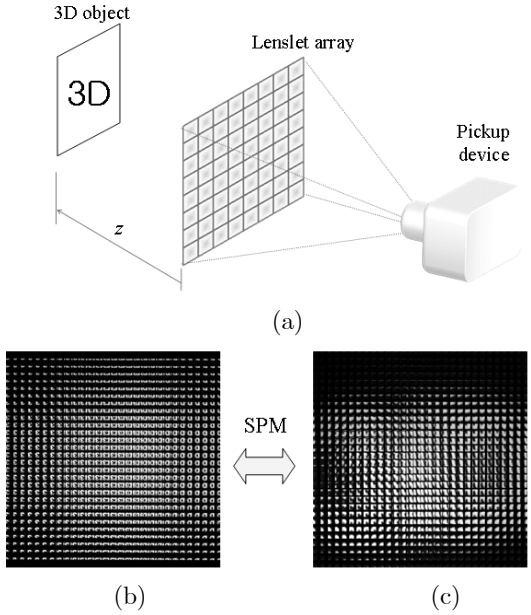


FIG. 5. (a) Optical pickup setup (b) Captured EIA (b) Depth-converted EIA using SPM

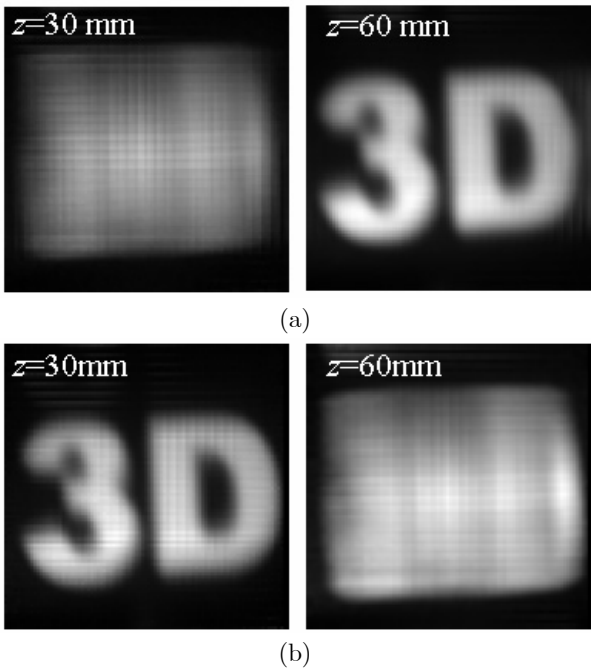


FIG. 6. Reconstructed images at the distances of 30 mm and 60 mm (a) Original EIA (b) Depth-converted EIA.

Using this SPM structure, the captured EIA was mapped into the depth-converted EIA. The resultant EIA having $900 \times 900$ pixels is shown in Fig. 5(c). It can be seen from Fig. 5 that our designed SPM model provides a function of depth conversion well. This SPM process was only 0.35 sec, which is very small compared with that of VCR process as shown in Fig. 4, because of the simple pixel mapping.

Next, we reconstructed the computationally 3D object images at the distance of $z = 30$ and 60 mm by using the VCR process as given in Eqs. (2) and (3). The reconstructed images are shown in Fig. 6. Figure 6(a) and 6(b) are the images reconstructed using the original EIA and our depth-converted EIA, respectively. In case of using the original EIA, the clear images of the 3D object were reconstructed at the distance of 60 mm where the 3D object was located originally. On the other hand, when using the depth-converted EIA in the proposed method the clear image was found at 30 mm. This shows that our method can move the ROP distance near the lenslet array effectively. According to the Fig 4, the computational time was approximately 187 sec when the original EIA was used, while our method was approximately 54 sec to reconstruct the clear image. Therefore the proposed method can significantly reduce the computational time by approximately 3.5 times. Therefore, it is seen that the proposed method can be an effective solution to reduce the computational cost.

## IV. CONCLUSION

In conclusion, we proposed a novel CII to reduce the computational cost dramatically. We applied a computational depth conversion technique to the conventional CII method. This function of depth conversion provided us with moving a far object near a lenslet array and then reducing the computational cost of reconstructed 3D image for far objects. From the preliminary experiment we demonstrated our CII method effectively. Therefore the proposed method can be usefully applied to the 3D visualization and pattern recognition.

## ACKNOWLEDGMENT

This research was supported by the MKE (Ministry of Knowledge Economy), Korea, under the ITRC (Information Technology Research Center) support program supervised by the IITA (Institute of Information Technology Assessment) (IITA-2008-C1090-0801-0018).

## REFERENCES

[1] G. Lippmann, "La photographic intergrale," *Comptes-Rendus Acad. Sci.*, vol. 146, pp. 446-451, 1908.
[2] A. Stern and B. Javidi, "Three-dimensional image sensing, visualization, and processing using integral imaging," *Proceedings of the IEEE*, vol. 94, no. 3, pp. 591-607, 2006.
[3] B. Lee, S. Y. Jung, S.-W. Min, and J.-H. Park, "Three-dimensional display by use of integral photography with dynamically variable image planes," *Opt. Lett.*, vol. 26,

no. 19, pp. 1481-1482, 2001.

[4] J. -S. Jang and B. Javidi, "Improved viewing resolution of three-dimensional integral imaging by use of nonstationary micro-optics," *Opt. Lett.*, vol. 27, no. 5, pp. 324-326, 2002.

[5] R. Martinez-Cuenca, A. Pons, G. Saavedra, M. Martinez-Corral, and B. Javidi, "Optically-corrected elemental images for undistorted Integral image display," *Opt. Exp.*, vol. 14, no. 21, pp. 9657-9663, 2006.

[6] D.-H. Shin and H.-Yoo, "Image quality enhancement in 3D computational integral imaging by use of interpolation methods," *Opt. Exp.*, vol. 15, no. 19, pp. 12039- 12049, 2007.

[7] H. E. Ives, "Optical properties of a Lippmann lenticulated sheet," J. Opt. Soc. Am., vol. 21, no. 3, pp. 171-176, 1931.

[8] J. Arai, F. Okano, H. Hoshino, and I. Yuyama, "Gradient-index lens-array method based on real-time integral photography for three-dimensional images," *Appl. Opt.*, vol. 37, no. 11, pp. 2034-2045, 1998.

[9] Y. Igarishi, H. Murata, and M. Ueda, "3D display system using a computer-generated integral photograph," *Jpn. J. Appl. Phys.*, vol. 17, no. 9, pp. 1683-1684, 1978.

[10] B. Lee, S.-W. Min, S. Jung, and J.-H. Park, "A three-dimensional display system based on computer-generated integral photography," *J. Soc. 3D Broadcase. Imag.*, vol. 1, no. 1, pp. 78-82, 2000.

[11] M. Martinez-Corral, B. Javidi, R. Martinez-Cuenca, and G. Saavedra, "Formation of real, orthoscopic integral images by smart pixel mapping," *Opt. Exp.*, vol. 13, no. 23, pp. 9175-9180, 2005.

[12] S. -H. Hong, J. -S. Jang, and B. Javidi, "Three-dimensional volumetric object reconstruction using computational integral imaging," *Opt. Exp.*, vol. 12, no. 3, pp. 483-491, 2004.

[13] H. Yoo and D. -H. Shin, "Improved analysis on the signal property of computational integral imaging system," *Opt. Exp.*, vol. 15, no. 21, pp. 14107-14114, 2007.

[14] S.-H. Hong and B. Javidi, "Distortion-tolerant 3D recognition of occluded objects using computational integral imaging," *Opt. Exp.*, vol. 14, no. 25, pp. 12085-12095, 2006.

[15] J. -B. Hyun, D. -C. Hwang, D. -H. Shin, and E. -S. Kim, "Curved computational integral imaging reconstruction technique for resolution-enhanced display of three-dimensional object images," *Appl. Opt.* vol. 46, no. 31, pp. 7697-7708, 2007.